QUANTITATIVE ANALYSIS OF THE VOID SIZE DISTRIBUTION IN THE LCRS AND IN CDM MODELS

V. MÜLLER, S. ARBABI-BIDGOLI
Astrophysikalisches Institut Potsdam, D-14482 Potsdam, Germany
E-mail: vmueller@aip.de, sarbabi@aip.de

We have analyzed the size distribution of voids in 2D slices of the Las Campanas Redshift Survey (LCRS). The characteristic sizes show a scaling $D = D_0 + \nu\lambda$ with the mean galaxy separation λ. Comparison with mock samples of the LCRS in 2D and 3D, using various simulations, cosmologies and galaxy identification schemes, gives a similar scaling, but with steeper slope and a lack of large voids. Best results are obtained for dark matter halos in a ΛCDM model.

1 Voids in the LCRS

The appearence of large voids in the galaxy distribution of extended galaxy surveys as the Las Campanas Redshift Survey (LCRS, Shectman et al. [1]) was one of the most spectacular findings characterizing the large-scale matter distribution of the universe. We expect large voids due to the matter outflow from positive primordial potential perturbations [2,3]. A second mechanism for the lack of galaxies in voids is the lower probability of galaxy formation in underdense regions known as biasing. Recently, Friedmann and Piran [4] presented a simple model for void formation based on the probability distribution of spherical underdense regions in the universe, and the less abundance of density peaks therein. There it was aimed to explain that in recent redshift surveys voids have radii between 13 and 30 h^{-1}Mpc, occupy 50% of the volume, and that the probability of larger voids falls off exponentially. Since the theoretical conclusions are based on a simple analytical model, and since galaxy surveys before LCRS were not extended enough to get reliable void statistics, we have undertaken a new quantitative study of voids in the LCRS and in numerical simulations [5]. Here this analysis is evaluated and compared with theoretical expectations.

In our analysis [5] we have used automatic void finders in 2D. Voids are identified as connected empty cells on a grid, where first square base voids are identified, and then boundary layers are added if they are empty and larger than 2/3 of the previous extension. The void finder starts with the search for the largest voids. The algorithm was first described and tested in 2D using slices through the CfA galaxy redshift survey by Kauffmann & Fairall [7].

From the LCRS we have selected 14 volume limited subsets in different radial ranges of the six narrow slices, projected them into the central planes and corrected for variations in the sampling fraction. In Fig. 1 the void distribution of such sets is shown which illustrates that we got a large number of voids in each data set, and that the voids cover smoothly the surface of the slice, with no obvious inhomogeneities or biasing by boundary effects or radial gradients. To emphasize the importance of large voids, we constructed the size distribution as cumulative coverage of the survey area with voids. Results are shown in Fig. 2. In the left pannel we overplot the void distributions of all 14 samples in normalizing them

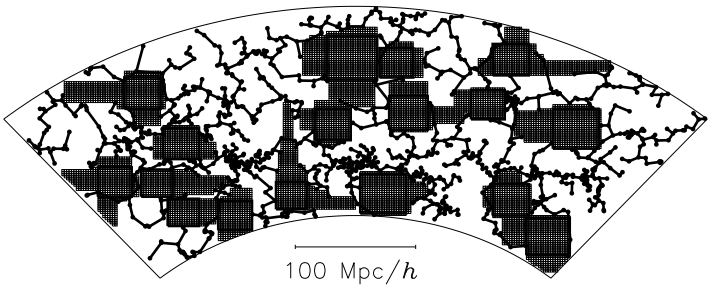

Figure 1. Large voids in a well sampled LCRS slice. Voids are empty regions marked by square base voids and rectangular extensions. Galaxies are shown by dots connected with the minimal spanning tree to emphasize the overdense regions

with the median void sizes from each sample. The thick lines show the results from the best sampled part of the survey. Altogether we get a nice convergence to a mean behavior shown by a smooth parametric fit. Also the derivative is shown in comparison with the distribution of voids in random point distributions which shows the main result of the gravitational clustering of galaxies in overdense regions: The relative abundence both of large voids and of small voids in the data is larger than in the random point distributions (the dashed lines).

2 Comparison with simulations

We have compared the LCRS voids with cold dark matter simulations in spatially flat Λ-term cosmology (ΛCDM, $\Omega_0 = 0.3$) and in open models (OCDM, $\Omega_0 = 0.5$). PM simulations were performed in 500 h^{-1}Mpc boxes using 300^3 particles and a threshold bias prescription to identify 'galaxies' with single particles. In addition we analyzed P3M simulations in 280 h^{-1}Mpc boxes and with 256^3 particles, a friend-of-friend halo finder, and a procedure to split off unvirialized halos that result from particle clumps merged by numerical effects. The mock samples in the different simulations fit well the 2-point correlation function of the LCRS as already shown in Tucker et al. [8]. In the right pannel of Fig. 3, we compare the real space correlation function of the mock samples with the reconstructed 3D correlation function of APM galaxies [9]. The mock samples provide good fits to the observations especially on large scales.

The cumulative void size distribution of ten OCDM mock samples is shown in the right pannel of Fig. 2 together with the variance range. Obviously this model has difficulty in matching the void distribution for a large range from 15 to 35 h^{-1}Mpc. The ΛCDM fits better, but it also seems to underestimate the size of the largest voids.

3 Scaling Relation

The 14 analyzed volume-limited data sets show variations in the galaxy densities which are due to different absolute magnitude cuts and different sampling fractions.

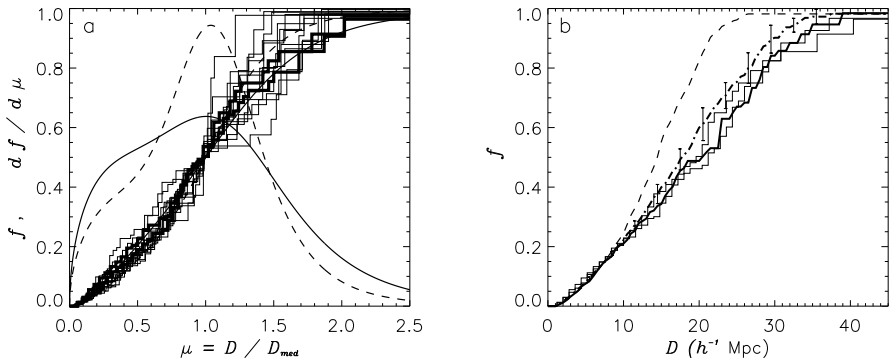

Figure 2. Cumulative area covered by voids as function of the size D compared to voids in a random point distribution (*dashed lines*). (**a**) LCRS void sizes measured in terms of the median size together with a fit (*solid line*) and its derivative. (**b**) LCRS histograms compared to mock samples of OCDM (*dash-dotted line with errors*) and ΛCDM (*thick line*)

Table 1. Parameters of the similarity relation of the void size distribution.

data	median		lower quartile		upper quartile	
	D_0 h^{-1}Mpc	ν	D_0 h^{-1}Mpc	ν	D_0 h^{-1}Mpc	ν
LCRS	11.8 ± 2.9	1.1 ± 0.2	5.7 ± 1.6	0.9 ± 0.1	16.8 ± 2.9	1.5 ± 0.2
Poisson	0.9 ± 1.0	1.8 ± 0.1	0.9 ± 0.3	1.2 ± 0.1	2.1 ± 0.5	2.1 ± 0.1
ΛCDM	7.6 ± 0.9	1.5 ± 0.1	2.9 ± 1.2	1.1 ± 0.1	14.2 ± 1.2	1.8 ± 0.1
OCDM	10.7 ± 1.8	1.2 ± 0.2	4.8 ± 0.6	1.0 ± 0.1	15.7 ± 2.7	1.8 ± 0.2

We already showed [5] that differences in the magnitude ranges have negligible influence on the size distribution of voids. So we ascribed the differences in the parameters of the void distributions to variations in the galaxy sampling densities. We measured it by the mean galaxy separation λ. In analyzing both data and mock samples, we found a characteristic scaling relation for the mean void sizes that cover 25%, 50% and 75% of the survey area. This scaling is a simple linear relation $D = D_0 + \nu\lambda$, with size $D_0 = (6, 12, 17)\, h^{-1}$Mpc and slope $\nu = (0.9, 1.1, 1.5)$ for 25%, 50% and 75% of void coverage, cp. Table 1.

In Fig. 3 we show that the scaling relations in simulated OCDM mock samples are steeper, $\nu_{model} > \nu_{data}$. It is even steeper for the ΛCDM model as seen in Table 1. According to our analysis, the median size of voids is larger than reported from earlier surveys [4]. The largest voids have a size of $D_{max} \approx 50\, h^{-1}$Mpc not met in simulations. Tests with mock samples indicate that the 2D-void size distributions in LCRS slices have a fixed ratio to the 3D-voids. Further, we have shown that large voids increase in size by 10 % in redshift space, but small voids remain unchanged, cp. also [6]. Our mock samples were always analyzed in redshift space.

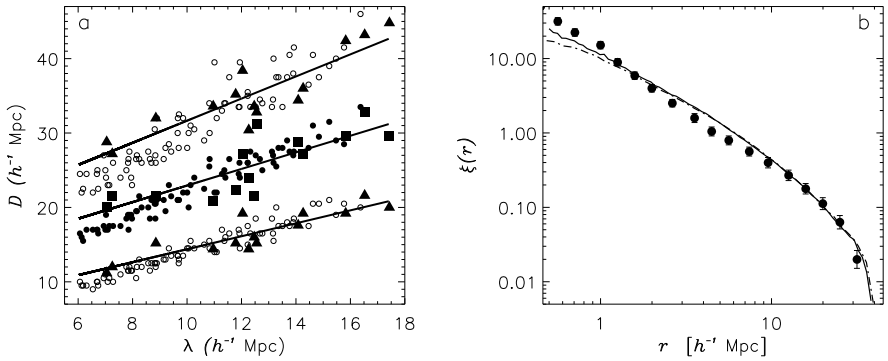

Figure 3. (**a**) Median (*squares*) and quartiles (*triangles*) of the void sizes versus the galaxy separation λ and the scaling relations as thick lines. The circles (*filled for the median*) for the OCDM mock samples show smaller void sizes for low λ. (**b**) Comparison of the real space two-point correlation function in the APM survey compared with the ΛCDM (solid line) and OCDM (dashed-dotted line) mock samples.

4 Discussion

The void statistics provide important characteristics of the galaxy distribution in low to medium dense regions where the correlation function is less sensitive. The self-similarity of the size distribution of samples with different mean galaxy separations culled by random dilutions and the scaling relation of the percentile sizes represent a genuine feature of hierarchical clustering. The discrepancy of the simulated void distribution to observations requires a stronger biasing of simulated galaxies and a higher concentration of them in superclusters, as has also been seen by analyzing overdensity regions with the minimal spanning tree technique illustrated in Fig. 1, cp. Doroshkevich et al. [10].

References

1. S. A. Shectman, S. D. Landy, A. Oemler, D. L. Tucker, H. Lin, R. P. Kirshner, P. L. Schechter , *ApJ* **470**, 172 (1996).
2. S. Madsen, A.G. Doroshkevich, S. Gottlöber, V. Müller, *A&A* **329**, 1 (1998).
3. J. Lee, S. Shandarin, *ApJ* **505**, L75 (1998).
4. Y. Friedmann, T. Piran, *ApJ* in press, astro-ph/0009320 (2000).
5. V. Müller, S. Arbabi-Bidgoli, J. Einasto, D. Tucker, *MNRAS* **325**, 280 (2000).
6. J.D. Schmidt, B.S. Ryden, A.L. Melott, *ApJ* **546**, 609 (2001).
7. G. Kauffmann, A.P. Fairall 1991, *MNRAS* **248**, 313 (1991).
8. D.T. Tucker, A. Oemler, R.P. Kirshner, H. Lin, S.A. Shectman, S.D. Landy, P.L. Schechter, V. Müller, S. Gottlöber, J. Einasto, *MNRAS* **285**, L5 (1997).
9. C.M. Baugh, *MNRAS* **280**, 267 (1996).
10. A.G. Doroshkevich, V. Müller, J. Retzlaff, V. Turchaninov, *MNRAS* **306**, 575 (1999).